

Percolation on two-dimensional elastic networks with rotationally invariant bond-bending forces

Shechao Feng

*Schlumberger-Doll Research, P. O. Box 307, Ridgefield, Connecticut 06877
and Department of Physics, Harvard University,
Cambridge, Massachusetts 02138*

P. N. Sen

Schlumberger-Doll Research, P. O. Box 307, Ridgefield, Connecticut 06877

B. I. Halperin and C. J. Lobb

*Department of Physics and Division of Applied Sciences, Harvard University,
Cambridge, Massachusetts 02138*

(Received 21 August 1984)

The behavior at the percolation threshold of a two-dimensional elastic network, involving both central and *rotationally invariant* bond-bending forces, is studied by numerical simulations and finite-size scaling analysis. A critical exponent $f \geq 3$ is found that is much higher than the corresponding exponent $t \approx 1.3$ for the electrical conductivity of a resistor network at percolation. This new result supports the previous result from a purely central force model and a mean-field-type analysis of the present model. If the bond-bending-force constant is not smaller than the stretching-force constant, an interesting crossover from a conductivity-like scaling behavior to the elastic one is observed as the system size is increased.

The purpose of this paper is to show that the elastic modulus near the percolation threshold of a *rotationally invariant* model with bond-bending forces is governed by an exponent f which is different from the corresponding exponent t for the electrical conductivity. This result was found previously for a purely central force nearest-neighbor model,¹ which is particularly easy to study by numerical simulations, but which is also a somewhat pathological case in some respects. In this Rapid Communication we study a more realistic model, including both central and bond-bending forces, using numerical simulations, and finite-size scaling analysis. Bond-bending forces were considered by Harris² and by Kantor and Webman³ in an analysis using mean-field and scaling arguments, which also gave an estimate of f much greater than t .⁴ A recent experimental study⁵ of the elastic properties of metallic plates with punched holes also leads to a large exponent f .

The principal result of our calculation is that the elastic modulus exponent of the bond-bending model, f , is again much greater than the conductivity exponent t in two dimensions. Our extrapolation of the data, and subjective estimate of the uncertainty, give $f \approx 3.3 \pm 0.5$, which is in good agreement with the result of Kantor and Webman³ and which is consistent, in the sense of having overlapping error bars, with the previous result for the central force elastic percolation model,¹ $f_{\text{cen}} \approx 2.4 \pm 0.4$. At this point, however, we cannot rule out the possibility that the bond-bending force model and the purely central force model belong to two distinct universality classes, because of the peculiarities of the central force model. In fact, Lemieux, Breton, and Tremblay⁶ have recently reported the results of a calculation which gave a much lower value $f_{\text{cen}} \approx 1.05 \pm 0.1$.

To be more explicit, the bulk modulus K and shear modulus N of the entire network go to zero as the fraction of the occupied bonds p falls below a critical value. For the case of *purely central forces* [$\gamma = 0$ in (3) below], the result

of Ref. 1 for a triangular lattice was that as p approaches the value $p_{\text{cen}} \approx 0.58$

$$K, N \sim (p - p_{\text{cen}})^{f_{\text{cen}}}, \quad (1)$$

with the value of f_{cen} quoted above. The critical concentration p_{cen} is *greater* than the geometric connectivity threshold p_c , which has the value $p_c = 0.3473$ for the triangular lattice, because there exist "floppy regions,"⁷ which are connected but cannot transmit an elastic force, in the central force model.

When bond-bending forces are included [$\gamma \neq 0$ in (3)], the elastic threshold moves down to p_c , and we may write

$$K, N \sim (p - p_c)^f. \quad (2)$$

In the present work, we employ a two-dimensional square lattice, where the exact value of $p_c = 0.5$ is known from a duality theorem.⁸

The purely central force model is rotationally invariant, but suffers from a few peculiarities, as follows: (a) the model has an elastic threshold of $p_{\text{cen}} = 1$ on all hypercubic lattices; (b) the significance of the straight bond chains in transmitting elastic forces is ambiguous, since, in a non-linear model, the straight bonds could "buckle" under compression but not under extension;⁹ (c) the dynamical matrix of a given pair of bonds, and for many more complicated configurations, is not invertible. The inclusion of the rotationally invariant bond-bending forces in the present study removes these peculiarities. In any case, since naturally occurring disordered systems cannot be precisely represented by any simple lattice model, it seems desirable to explore a variety of different systems so that one can develop a systematic understanding of the various universality classes involved in the elastic percolation.

We now describe the bond-bending elastic network model. Consider a two-dimensional (2D) square lattice. The poten-

tial energy of the lattice is given by

$$V = \frac{\alpha}{2} \sum_{\langle ij \rangle} [(\bar{U}_i - \bar{U}_j) \cdot \hat{r}_{ij}]^2 g_{ij} + \frac{\gamma}{2} \sum_{\langle ijk \rangle} (\delta\Theta_{ijk})^2 g_{ij} g_{ik} \quad (3)$$

Here, \bar{U}_i and \bar{U}_j are displacements of node i and node j ; $g_{ij} = 1$ for the bonds that are occupied, with a probability p , and $g_{ij} = 0$ for the bonds that are empty, with a probability $1 - p$; \hat{r}_{ij} is the unit vector from node i to node j . The sums are, respectively, over all bonds and over all pairs of bonds with a site in common. The bond-bending forces between two connected nearest-neighbor occupied bonds ij and ik are given in terms of the change in angle $\delta\Theta_{ijk}$ at node i , which is expressed in turn as a linear function of \bar{U}_i , \bar{U}_j , and \bar{U}_k . This model is essentially the same as the Kirkwood model¹⁰ and the Keating model,¹¹ except that we now include the bending of 180° bonds. This is to be contrasted with the situation when a rotationally noninvariant, and therefore unphysical, Born model was used in describing the angular forces.¹ With the Born model, the percolation threshold also returned to p_c , the ordinary connectivity threshold, but, in contrast to above, the critical exponent became equal to t . In Ref. 1, the Born model was used to illustrate only qualitatively the crossover from a central force-dominated behavior near p_{cen} to angular force-dominated behavior near p_c .

The finite sample size L is an obstacle towards getting good critical exponents in a direct simulation, because the coherence length $\xi \sim (p - p_c)^{-\nu}$ diverges as p approaches p_c . We employ the finite-size scaling calculational scheme¹² following the work of Lobb and Frank^{13,14} on the percolative conduction problem. In this approach, we fix p at the exact value of p_c , and extract the critical exponents from the dependence of the elastic moduli and conductivity, when properly averaged, on the sample size. To be specific, we write for $p = p_c$

$$K, N \sim L^{-f/\nu} [a_1 + a_2 g_f(L)] \quad (4)$$

$$\Sigma \sim L^{-t/\nu} [b_1 + b_2 g_t(L)] \quad (5)$$

Here, Σ is the conductivity of the same network, with unit conductance for the present bonds, and zero conductance for the missing ones, and a_1, a_2, b_1, b_2 are constants, and the functions $g_f(L)$ and $g_t(L)$ go to zero for large L . Some possible forms for $g_t(L)$ have been mentioned in Ref. 14. The finite-size scaling has also been used by several other authors.¹⁵

Our calculation is carried out as follows. First we generate a square lattice of height L and width $L + 1$, with randomly occupied nearest-neighbor bonds with probability $p = p_c = \frac{1}{2}$. In 50% of the realizations, the two vertical edges are not connected, and these realizations are disregarded. In the remaining cases, a sparse matrix inversion solving routine (courtesy of the Computer Science Department of Yale University)¹⁶ is used to solve for all the displacements in the system, with the boundary condition that we specify constant x displacements on each of the vertical edges while there are no normal forces at the horizontal edges and no tangential forces at any boundary. Then the solutions are used to obtain the forces on the boundary and, hence, the Young's modulus Y of the system for stress along the x axis. (We expect that all the elastic moduli should all vanish with the same exponent f as one approaches p_c , so only Y is calculated in this work.) Many realizations of the random configuration are generated and

the above calculations repeated in order to achieve good statistics. Three different means of the data—the arithmetic mean $(1/n) \sum_i^n Y_i$, the geometric mean $(\prod_i^n Y_i)^{1/n}$, and the harmonic $[(1/n) \sum_i^n Y_i^{-1}]^{-1}$ —are then calculated for the Young's modulus and the conductivity. The entire procedure is repeated for many different values of L , and (4) and (5) are subsequently used to extract the critical exponents.

A useful way to display the data is shown in Figs. 1 and 2 for the parameters $\gamma/\alpha = 1$ and $\gamma/\alpha = 0.1$, respectively. By plotting $\ln(1/Y)/\ln(L)$ against $1/\ln(L)$, the y intercept of the asymptotic straight lines becomes f/ν , as can be seen easily from (4). Both sets of data, and all three means, should yield the same value of f/ν . Indeed, if one extrapolates the data in Figs. 1 and 2 by eye to $1/\ln(L) = 0$, all three lines converge roughly to a value marked by a star on the y axis. It is to be noted, however, that the data with $\gamma = 0.1\alpha$ in Fig. 2 are straighter than in Fig. 1, so we have used these data for detailed curve fitting to (4). A marker (cross) for the value of t/ν is also shown on the figures for the purpose of comparison.

Our method of fitting has been described elsewhere.¹⁴ With much larger size lattices and better statistics, it was possible in the conductivity problem to determine t/ν to within a percent, and to choose between various possible forms for the correction $g_t(L)$. Since the present data span a smaller range of L and are less accurate, it was not possible to distinguish between various forms for $g_f(L)$, but fortunately, the value inferred for exponents does not seem to depend very strongly on the choice of the correction function. In the final fitting, therefore, we used $g_f(L) = 1/\ln(L)$ for convenience. Fits of this form were performed using all of the data points ($L = 3-50$) and with some of the lower L points removed ($L = 4-50, L = 6-50, L = 8-50$) to get a sense for the scatter in the data. All such fits were within 0.4 of $f/\nu = 2.5$ which, using $\nu = \frac{4}{3}$, gives the value quoted above, $f = 3.3 \pm 0.5$.

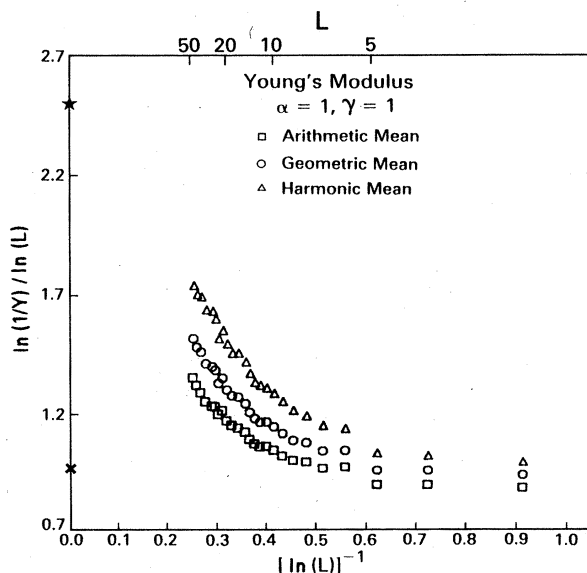


FIG. 1. Plot of $\ln(1/Y)/\ln(L)$ against $1/\ln(L)$ for $p = p_c = 1/2$, $\alpha = \gamma = 1$, 800 realizations for each L , and $3 < L < 50$. The star marked on the y axis is the extrapolated value of f/ν , and the cross corresponds to the value of t/ν . Note the change in slope at $L \approx 15$.

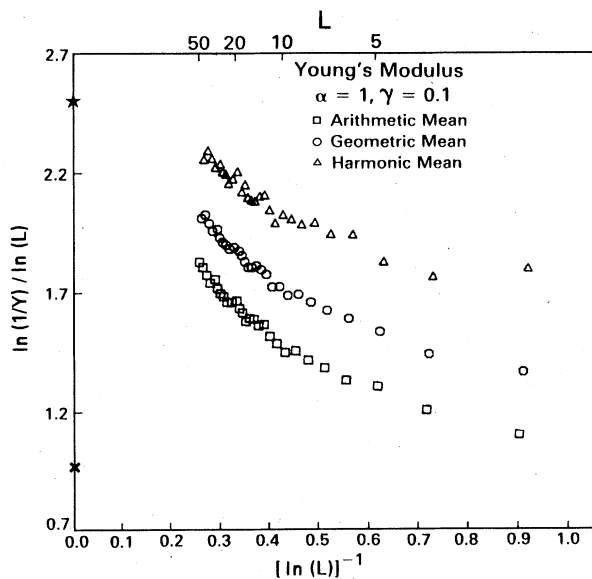


FIG. 2. Same as Fig. 1, but with $\alpha = 1$ and $\gamma = 0.1$.

The error estimated here is subjective, and of course we cannot totally rule out the possibility that data for larger values of L may show a change in behavior and lead to a value of f outside of our error bars.

Conductivity data generated from the same Monte Carlo realizations as used in Figs. 1 and 2 have been analyzed as above with the result $t/\nu = 0.96 \pm 0.05$, in good agreement with the more precise previous work.¹⁴ The relatively poor accuracy of the elastic exponent reflects a greater scatter in the Young's modulus data than in the conductivity data for a given L . The scatter is also manifest in the larger discrepancies in the values of the three different means for Y than for Σ .

The general features of Figs. 1 and 2 can be *qualitatively* understood as follows. Near the percolation threshold, strongly bonded regions are connected by tenuous weak regions. The strong regions can be regarded as perfectly rigid, so the elastic properties near p_c are dominated by the weak regions. These weak regions are quasi one dimensional and thus can be modeled as tortuous chains.¹⁷ Using a slight modification of the reasoning of Ref. 3, we expect that the effective force constant E of such a chain is dominated by the bond-bending forces, and we may estimate $E \approx c^2\gamma/(R\xi^2)$, where R is the resistance of the chain, and c a constant. This expression for E is essentially the same as in Ref. 3, but with N , the number of bonds in a typical

chain, replaced by its resistance. As p approaches p_c , the coherence length $\xi \sim (p - p_c)^{-\nu}$ diverges, and the elastic constant of the system goes to zero as $Y \approx c^2\gamma\Sigma/\xi^2\alpha(p - p_c)^f$, with $f \approx t + 2\nu \approx 3.96$, which differs slightly from the estimate $f = 2\nu + 1$ in Eq. (16) of Ref. 3, and which is slightly larger than our Monte Carlo result. On the other hand, for any fixed chain length (or fixed ξ) the above argument will break down if γ/α is sufficiently large. Specifically, if γ/ξ^2 is greater than α , it will cost less energy to accomplish a displacement of the chain ends of adjusting the length of bonds parallel to the stress, rather than bending bond angles; we then find in this case that $E \approx 2\alpha/R$ and, hence, $Y \approx 2\alpha\Sigma\alpha(p - p_c)^t$. For values of $\gamma/\alpha \geq 2c^{-2}$, we, therefore, expect two effective exponent regimes: namely, the conductivity-like scaling regime at low values of L and the elastic scaling regime at high values of L , with a crossover occurring at $L \approx c(\gamma/\alpha)^{1/2}$. In Fig. 1, for $\alpha = \gamma$, we see such a behavior for $L \approx 15$, which suggests a value $c \approx 15$, a number not unreasonable if the chain sizes are of the order $\xi/10$, and the typical chain widths are slightly larger than one lattice constant. In Fig. 2, for $\gamma/\alpha = 0.1$ we see a reasonably straight line behavior for all values of $L \geq 4$, which is consistent with the interpretation just given. [We have also obtained data for the case $\gamma/\alpha = 2$ (not shown) which exhibited a crossover behavior similar to that in Fig. 1 with the crossover length L at about 20, and the data at low L extrapolate to a value of about $t/\nu \approx 1$, as expected from the above argument.]

We note that for fixed bond-bending constant γ , we can take the limit $\alpha \rightarrow \infty$ in our model and Y will remain finite for any fixed $p < 1$. Thus, in the region of interest to us ($L > 3$), data for Y/γ in the limiting case $\gamma/\alpha \rightarrow 0$ should be very similar to the case $\gamma/\alpha = 0.1$ which is represented in Fig. 2.

The great sensitivity of the elastic constant to the physical size of chainlike regions should also explain the large scatter of the data for Y , compared with the data for Σ on the same set of realizations, for given L .

Note added in proof. After we submitted this paper we received a report of work prior to publication from D. J. Bergman, who also studied the same problem and came to similar conclusions.

We are grateful for useful discussions with E. Guyon, H. Herrmann, C. Henley, T. J. Lasseter, J. Koplik, H. E. Stanley, M. F. Thorpe, J. Vannimenus, A.-M. S. Tremblay, and J. R. Banavar. Work at Harvard was supported in part by the National Science Foundation through the Harvard Materials Research Laboratory.

¹S. Feng and P. N. Sen, Phys. Rev. Lett. **52**, 216 (1984).

²A. B. Harris (unpublished).

³Y. Kantor and I. Webman, Phys. Rev. Lett. **52**, 1891 (1984).

⁴The inequality $f \geq t$ has also been obtained for a Sierpinski gasket model of the percolating backbone by D. J. Bergman and Y. Kantor, Phys. Rev. Lett. **53**, 511 (1984).

⁵L. Benguigui (unpublished).

⁶M. A. Lemieux, P. Breton, and A.-M. S. Tremblay (unpublished).

⁷cf. M. F. Thorpe, J. Non Cryst. Solids **57**, 355 (1983).

⁸M. F. Sykes and J. W. Essam, J. Math. Phys. **5**, 1117 (1964).

⁹S. Feng, M. F. Thorpe, and E. Garboczi (unpublished).

¹⁰J. G. Kirkwood, J. Chem. Phys. **7**, 506 (1939).

¹¹P. N. Keating, Phys. Rev. **152**, 774 (1966).

¹²M. E. Fisher, in *Critical Phenomena*, edited by M. S. Green, Enrico Fermi Summer School Course No. LI (Academic, New York, 1972) pp. 1-99.

¹³C. J. Lobb and D. J. Frank, J. Phys. C **12**, L827 (1979).

¹⁴C. J. Lobb and D. J. Frank, Phys. Rev. B **30**, 4090 (1984).

¹⁵A. K. Saryachev and A. P. Vinogradoff J. Phys. C **14**, L487 (1981); C. D. Mitescu, M. Allain, E. Guyon, and J.-P. Clerc, J. Phys. A **15**, 2523 (1982); B. Derrida and J. Vannimenus, *ibid.* **15**, 2523 (1981); J. Rousseng, J. P. Clerc, G. Giraud, E. Guyon, and

- C. D. Mitescu, *J. Phys. C* **11**, 1311 (1978); A. Sur, J. L. Lebowitz, J. Marro, M. H. Kalus, and S. Kirkpatrick, *J. Stat. Phys.* **15**, 345 (1976); C. D. Mitescu and M. J. Musof, *J. Phys. (Paris) Lett.* **44**, L679 (1983); J. P. Straley, *J. Phys. C* **10**, 1903 (1977); M. Sahimi, B. D. Hughes, L. E. Scriven, and H. T. Davis, *ibid.* **16**, L521 (1983); M. Sahimi, *ibid.* **17**, L355 (1984); E. S. Kirkpatrick, in *III Condensed Matter*, edited by R. Balian, R. Maynard, and G. Toulouse (North-Holland, New York, 1979).
- ¹⁶S. C. Eisenstat, M. C. Gursky, M. H. Schultz, and A. H. Sherman, Yale University Research Report No. 112, 1983 (unpublished).
- ¹⁷A. Coniglio, *Phys. Rev. Lett.* **46**, 250 (1981).